Spherical Radial Basis Function Algorithms for Gravity Field Approximation

PAGravf4.5; https://www.zcyphygeodesy.com/en/
ZHANG Chuanyin; zpmzsyzcy1968@163.com
Chinese Academy of Surveying & Mapping
March 2026, Beijing, 100830, China

Classical spatial gravity field boundary value theory relies on a single type of observation gravity field element on a single boundary surface. In contrast, spectral domain gravity field approximation theory does not involve boundary surfaces or boundary value conditions. It can directly approximate the all-element gravity field using multi-source heterogeneous observations via the Least Squares Method, making it the mainstream approach in modern physical geodesy. This section introduces the theory and methodology of Spherical Radial Basis Function (SRBF) spectral domain approximation.

7.10.1 Representation of the External Disturbing Potential Using SRBFs

The disturbing potential $T(\boldsymbol{x})$ at an external point $\boldsymbol{x}$ can be expressed as a linear combination of fully normalized surface spherical harmonics:

$$T(\boldsymbol{x}) = \frac{GM}{r}\sum_{n=1}^{N}\left(\frac{a}{r}\right)^n \sum_{m=-n}^{n}\bar{F}_{nm}\bar{Y}_{nm}(\boldsymbol{e}) \tag{10.1}$$

where $\boldsymbol{x} = \boldsymbol{r}\cdot\boldsymbol{e} = r(sin\theta cos\lambda, sin\theta sin\lambda, cos\theta)$ represents geocentric spherical coordinates (θ, λ, r); $\bar{F}_{nm}$ are the fully normalized Stokes coefficients (geopotential coefficients); and a is the Earth's semi-major axis. The the normalized surface spherical harmonic basis functions $\bar{Y}_{nm}(\boldsymbol{e})$ are defined on the sphere of radius a:

$$\begin{aligned}\bar{Y}_{nm}(\boldsymbol{e}) &= \bar{P}_{nm}(cos\theta)cosm\lambda, \quad \bar{F}_{nm} = \delta\bar{C}_{nm}, \quad m \geq 0\\ \bar{Y}_{nm}(\boldsymbol{e}) &= \bar{P}_{n|m|}(cos\theta)sin|m|\lambda, \quad \bar{F}_{nm} = \bar{S}_{n|m|}, \quad m < 0\end{aligned} \tag{10.2}$$

where $\bar{P}_{nm}(cos\theta)$ is the fully normalized associated Legendre function; n is the degree and m is the order of the geopotential coefficients.

Equivalently, these basis functions $\bar{Y}_{nm}(\boldsymbol{e})$ can be defined on a Bjerhammar sphere of radius $\mathcal{R}$. Thus, $T(\boldsymbol{x})$ can also be written as:

$$T(\boldsymbol{x}) = \frac{GM}{r}\sum_{n=1}^{N}\left(\frac{\mathcal{R}}{r}\right)^n \sum_{m=-n}^{n}\bar{E}_{nm}\bar{Y}_{nm}(\boldsymbol{e}) \tag{10.3}$$

Here, $\mathcal{R} \in (a-\delta, a+\delta)$ with $\delta \ll a$. The relationship between coefficients is $a^n\bar{F}_{nm} = \mathcal{R}^n\bar{E}_{nm}$, and the surface spherical harmonics basis functions $\{\bar{Y}_{nm}(\boldsymbol{e})\}$ in Equations (10.3) and (10.1) is identical.

Alternatively, $T(\boldsymbol{x})$ can be represented as a linear combination of K Spherical Radial Basis Functions (SRBFs):

$$T(\boldsymbol{x}) = \frac{GM}{r}\sum_{k=1}^{K} d_k\Phi_k(\boldsymbol{x}, \boldsymbol{x}_k) = \frac{GM}{r}\sum_{k=1}^{K} d_k\Phi_k(\boldsymbol{x}, \psi_k) \tag{10.4}$$

where:

$\boldsymbol{x}_k = \mathcal{R}\cdot\boldsymbol{e}_k$: The SRBF node (center) on the Bjerhammar sphere.

ψ_k: The spherical angular distance between $\boldsymbol{x}_k$ and $\boldsymbol{x}$ (the argument of the SRBF).

d_k: The SRBF coefficient.

K: The number of nodes, i.e., the number of SRBF coefficients, determining the spatial resolution.

$\Phi_k(\boldsymbol{x}, \boldsymbol{x}_k) = \Phi_k(\boldsymbol{x}, \psi_k)$: The radial basis function for the disturbing potential, which can be abbreviated as $\Phi_k(\boldsymbol{x}) = \Phi_k(\boldsymbol{x}, \boldsymbol{x}_k)$.

The SRBF can be expanded into a Legendre series:

$$\Phi_k(\boldsymbol{x}, \boldsymbol{x}_k) = \Phi_k(\boldsymbol{x}, \psi_k) = \sum_{n=1}^{N} \phi_n P_n(\psi_k) = \sum_{n=1}^{N} \frac{2n+1}{4\pi} B_n \left(\frac{\mathcal{R}}{r}\right)^n P_n(\psi_k) \tag{10.5}$$

where ϕ_n is the n-th degree Legendre coefficient (or shape factor), characterizing the spectral properties of the SRBF, and $\mu = \mathcal{R}/r$ is the bandwidth parameter.

Note that N (maximum degree) and K (number of nodes) are independent parameters. The N in Equation (10.5) is the maximum degree of the Legendre functions. Although it is the maximum degree in the surface spherical harmonic expansion of the disturbing potential (Equation 10.3), there is no explicit functional relationship with K, the number of SRBF coefficients representing spatial resolution.

Substituting Eq. (10.5) into (10.4) and applying the Spherical Harmonic Addition Theorem:

$$P_n(\psi_k) = P_n(\boldsymbol{e}, \boldsymbol{e}_k) = \frac{4\pi}{2n+1} \sum_{m=-n}^{n} \bar{Y}_{nm}(\boldsymbol{e}) \bar{Y}_{nm}(\boldsymbol{e}_k) \tag{10.6}$$

$$T(\boldsymbol{x}) = \frac{GM}{4\pi r} \sum_{n=1}^{N} (2n+1) B_n \left(\frac{\mathcal{R}}{r}\right)^n \sum_{k=1}^{K} d_k P_n(\psi_k)$$

$$= \frac{GM}{4\pi r} \sum_{k=1}^{K} d_k \sum_{n=1}^{N} (2n+1) B_n \left(\frac{\mathcal{R}}{r}\right)^n P_n(\psi_k) \tag{10.7}$$

$$T(\boldsymbol{x}) = \frac{GM}{r} \sum_{n=1}^{N} B_n \left(\frac{\mathcal{R}}{r}\right)^n \sum_{m=-n}^{n} \sum_{k=1}^{K} d_k \bar{Y}_{nm}(\boldsymbol{e}) \bar{Y}_{nm}(\boldsymbol{e}_k) \tag{10.8}$$

yields the relationship between geopotential coefficients and SRBF coefficients:

$$\bar{F}_{nm} = \left(\frac{\mathcal{R}}{a}\right)^n \bar{E}_{nm} = B_n \left(\frac{\mathcal{R}}{a}\right)^n \sum_{k=1}^{K} d_k \bar{Y}_{nm}(\boldsymbol{e}_k) \tag{10.9}$$

This relation holds for global domain ($\psi_k \in [0, \pi)$). For local gravity field approximation, ψ_k acts analogously to the integration radius in spatial methods. The distribution and number K of SRBF centers determine the spatial degrees of freedom.

7.10.2 Suitable Spherical Radial Basis Functions for Gravity Field Approximation

SRBFs must satisfy Laplace's equation ($\Delta\Phi = 0$). Common harmonic kernels include the Point-Mass kernel, Poisson kernel, Radial Multipole kernel, and Poisson Wavelet kernel.

(1) Analytical Forms and Normalized Representation

Let $\boldsymbol{x}$ be the computation point and $\boldsymbol{x}_k$ the SRBF node on the Bjerhammar sphere $\Omega_{\mathcal{R}}$.

● Point-Mass Kernel: An inverse multiquadric (Newtonian) kernel.

$$\Phi_{IMQ}(\boldsymbol{x}, \boldsymbol{x}_k) = \frac{1}{L} = \frac{1}{|\boldsymbol{x} - \boldsymbol{x}_k|} \tag{10.10}$$

where: L is the spatial distance from $\boldsymbol{x}_k$ to $\boldsymbol{x}$. The point-mass function is also known as the Newtonian kernel function. Since $\Delta(1/L) = 0$, the point-mass kernel function $\Phi_{IMQ}(\boldsymbol{x}, \boldsymbol{x}_{\mathrm{k}})$ satisfies Laplace's equation.

● Poisson Kernel: Derived from the Poisson integral.

$$\Phi_P(\boldsymbol{x},\boldsymbol{x}_k) = -2r\frac{\partial}{\partial r}\left(\frac{1}{L}\right) - \frac{1}{L} = \frac{r^2 - r_k^2}{L^3} \tag{10.11}$$

● Radial Multipole Kernel (Order m):

$$\Phi_{RM}^m(\boldsymbol{x},\boldsymbol{x}_k) = \frac{1}{m!}\left(\frac{\partial}{\partial r_k}\right)^m \frac{1}{L} \tag{10.12}$$

Note: $m = 0$ yields the point-mass kernel: $\Phi_{IMQ}(\boldsymbol{x},\boldsymbol{x}_k) = \Phi_{RM}^0(\boldsymbol{x},\boldsymbol{x}_k)$.

● Poisson Wavelet Kernel (Order m):

$$\Phi_{PW}^m(\boldsymbol{x},\boldsymbol{x}_k) = 2(\chi_{m+1} - \chi_m), \quad \chi_m = \left(r_k\frac{\partial}{\partial r_k}\right)^m \frac{1}{L} \tag{10.13}$$

Note: $m = 0$ yields the Poisson kernel: $\Phi_P(\boldsymbol{x},\boldsymbol{x}_k) = \Phi_{PW}^0(\boldsymbol{x},\boldsymbol{x}_k)$.

(2) Computation of Spherical Radial Basis Functions

To highlight spectral properties and simplify multi-type data processing, SRBFs can be computed via their normalized Legendre series. A normalization coefficient Φ^0 is defined by evaluating the series at $\psi_k = 0$ ($P_n(1) = 1$):

$$\Phi^0 = \sum_{n=1}^N \frac{2n+1}{4\pi} B_n \mu^n \tag{10.14}$$

The Normalized SRBF is then:

$$\Phi_k(\boldsymbol{x},\boldsymbol{x}_k) = \frac{1}{\Phi^0}\sum_{n=1}^N \phi_n P_n(\psi_k) = \frac{1}{\Phi^0}\sum_{n=1}^N \frac{2n+1}{4\pi} B_n \mu^n P_n(\psi_k) \tag{10.15}$$

This normalization preserves the linear functional relationships between different gravity field elements (e.g., potential, anomaly, and disturbance).

Table 7.2: Disturbing Potential Spherical Radial Basis Functions and Their Legendre Coefficients

SRBF Type	Analytical Form Φ_k	Legendre Coeff. ϕ_n	Parameter B_n
Point mass kernel	$\frac{1}{L} = \frac{1}{\lvert x - x_k\rvert}$	μ^n	$\frac{1}{2n+1}$
Poisson kernel	$\frac{r^2 - r_k^2}{L^3}$	$(2n+1)\mu^n$	1
Radial multipole kernel (m)	$\frac{1}{m!}\left(\frac{\partial}{\partial r_k}\right)^m \frac{1}{L}$	$C_n^m \mu^{n-m}\ (n \geq m)$	$\frac{C_n^m}{2n+1}\mu^{-m}$
Poisson wavelet kernel (m)	$2(\chi_{m+1} - \chi_m)$ $\chi_m = \left(r_k\frac{\partial}{\partial r_k}\right)^m \frac{1}{L}$	$(-nln\mu)^m(2n+1)\mu^n$	$(-nln\mu)^m$

(3) Series Representation of Various Anomalous Field elements Using SRBFs

Based on the definitions of anomalous field elements, the parameterized forms of SRBFs for other field types can be derived from the SRBF expansion of the disturbing potential (Eq. 10.6). By applying appropriate differential operators, we obtain:

● Disturbing Potential (Height Anomaly):

$$T(\boldsymbol{x}) = \gamma\zeta(\boldsymbol{x}) = \frac{GM}{4\pi r}\sum_{k=1}^K d_k \sum_n (2n+1) B_n \left(\frac{\mathcal{R}}{r}\right)^n P_n(\psi_k) \tag{10.16}$$

● Gravity Disturbance:

$$\delta g(\boldsymbol{x}) = -\frac{\partial T}{\partial r} = \frac{GM}{4\pi r^2}\sum_{k=1}^K d_k \sum_n (2n+1)(n+1) B_n \left(\frac{\mathcal{R}}{r}\right)^{n-1} P_n(\psi_k) \tag{10.17}$$

● Gravity Anomaly:

$$\Delta g(\boldsymbol{x}) = \frac{GM}{4\pi r^2}\sum_{k=1}^{K} d_k \sum_n (2n+1)(n-1)B_n \left(\frac{\mathcal{R}}{r}\right)^{n-1} P_n(\psi_k) \tag{10.18}$$

- Vertical Deflection Components (ξ: North-South, η: East-West):

$$\xi(\boldsymbol{x}) = \frac{GM}{4\pi r^2 \gamma}\sum_{k=1}^{K} d_k \cos\alpha_k \sum_n (2n+1)B_n \left(\frac{\mathcal{R}}{r}\right)^{n} \frac{\partial P_n(\psi_k)}{\partial \psi_k} \tag{10.19}$$

$$\eta(\boldsymbol{x}) = \frac{GM}{4\pi r^2 \gamma}\sum_{k=1}^{K} d_k \sin\alpha_k \sum_n (2n+1)B_n \left(\frac{\mathcal{R}}{r}\right)^{n} \frac{\partial P_n(\psi_k)}{\partial \psi_k} \tag{10.20}$$

- Radial Disturbing Gravity Gradient:

$$T_{rr}(\boldsymbol{x}) = \frac{GM}{4\pi r^3}\sum_{k=1}^{K} d_k \sum_n (2n+1)(n+1)(n+2)B_n \left(\frac{\mathcal{R}}{r}\right)^{n-1} P_n(\psi_k) \tag{10.21}$$

where $\mu = \mathcal{R}/r$ is the bandwidth parameter, and α_k is the geodetic azimuth of ψ_k.

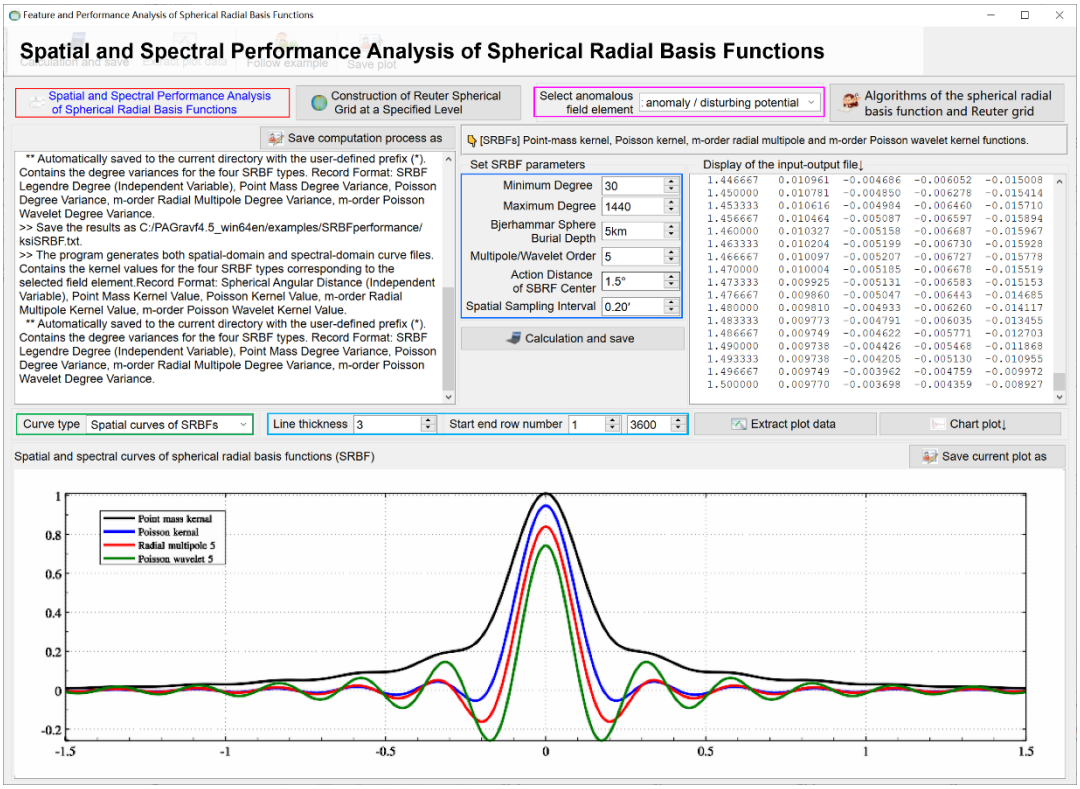

Figure 7.8: Calculation of curves of the four normalized SRBF types

Parameter Selection for Local Approximation:

In local gravity field modeling, a Remove-Restore technique is typically employed: medium-to-low frequency signals are removed using a reference global geopotential model, and residuals are approximated regionally. Consequently, the spectral bandwidth (range of degree n) and the domain of the argument ψ_k in Eqs. (10.16) – (10.21) depend critically on:

- The chosen reference global geopotential model.
- The target regional gravity field structure.
- The desired spatial resolution (controlled by the number of SRBF nodes K or the Reuter grid level Q).

These parameters should be optimized through empirical testing with actual gravity field observation data in target region.

(4) Reuter Grid Construction and Adaptive SRBF Node Design

A Spherical Equal-Area Reuter Grid provides a globally and regionally consistent framework for node distribution. Given a grid level Q, SRBF nodes (centers) are constructed such that their spatial density adapts to the distribution of observations. The level Q acts as the spatial resolution indicator, analogous to the maximum degree N_{max} of a global geopotential model.

● Unit Sphere Reuter Grid Algorithms

For an even integer level Q, the geocentric latitude interval $d\varphi$ and the latitude φ_i of the i-th row center are:

$$d\varphi = \frac{\pi}{Q}, \quad \varphi_i = -\frac{\pi}{2} + \left(i - \frac{1}{2}\right) d\varphi, \quad 1 \le i < Q \tag{10.22}$$

The number of cells J_i along the parallel at φ_i, the longitude interval $d\lambda_i$, and the approximate side length dl_i are:

$$J_i = \left[\!\left[\frac{2\pi cos\varphi_i}{d\varphi}\right]\!\right] = [\![2Qcos\varphi_i]\!], \quad d\lambda_i = \frac{2\pi}{J_i}, \quad dl_i = d\lambda_i cos\varphi_i \tag{10.23}$$

where $[\![\cdot]\!]$ denotes the floor function. Note that $dl_i \approx d\varphi$.

The relative area deviation ε_i from the equatorial cell area ds is:

$$\varepsilon_i = \frac{ds_i - ds}{ds} = \frac{dl_i - d\varphi}{d\varphi} = \frac{d\lambda_i}{d\varphi} cos\varphi_i - 1 \tag{10.24}$$

Typically, ε_i is negligible (order of 10^{-4}), ensuring near-perfect equal-area properties. For regional applications, indices i and J_i are restricted to the target latitude/longitude bounds, avoiding global grid computation.

● Adaptive SRBF Center Design

PAGravf4.5 implements an adaptive algorithm to align SRBF nodes with observation distribution density:

○ Construct a regional Reuter grid at level Q.

○ Count the number of effective observations j within each grid cell containing a potential SRBF node.

○ Pruning Rule: If j is below a user-defined minimum threshold, the corresponding SRBF node is discarded.

○ The remaining nodes form an adaptive SRBF network.

This ensures that SRBF node distribution mirrors observation distribution: regular grids yield regular nodes; irregular or clumped observations yield irregular nodes.

Global Node Count Estimate:

Setting $Q = N_{max}$, the total number of SRBF nodes K for a global grid satisfies:

$$K = \sum_{i=1}^{Q} J_i = \sum_{i=1}^{Q} [\![2Qcos\varphi_i]\!] > N_{maxn}(N_{maxn} + 2) \tag{10.25}$$

Thus, the number of SRBF coefficients slightly exceeds the number of spherical harmonic coefficients for equivalent resolution.

7.10.3 Local Gravity Field Approximation Using the Spectral Domain SRBF Method

Gravity field approximation is essentially a linear spatial transformation. Removing constant factors ($GM/(4\pi)$) and common radial terms ($1/r$) simplifies the observation equations without altering analytical relationships. Eqs. (10.16) – (10.21) simplify to:

$$\zeta(\boldsymbol{x}) = \frac{1}{\gamma}\sum_{k=1}^{K} d_k \sum_n (2n+1) B_n \mu^n P_n(\psi_k) \tag{10.26}$$

$$\delta g(\boldsymbol{x}) = \frac{1}{r}\sum_{k=1}^{K} d_k \sum_n (2n+1)(n+1) B_n \mu^{n-1} P_n(\psi_k) \tag{10.27}$$

$$\Delta g(\boldsymbol{x}) = \frac{1}{r}\sum_{k=1}^{K} d_k \sum_n (2n+1)(n-1) B_n \mu^{n-1} P_n(\psi_k) \tag{10.28}$$

$$\xi(\boldsymbol{x}) = \frac{1}{r\gamma}\sum_{k=1}^{K} d_k \cos\alpha_k \sum_n (2n+1) B_n \mu^n \frac{\partial P_n(\psi_k)}{\partial \psi_k} \tag{10.29}$$

$$\eta(\boldsymbol{x}) = \frac{1}{r\gamma}\sum_{k=1}^{K} d_k \sin\alpha_k \sum_n (2n+1) B_n \mu^n \frac{\partial P_n(\psi_k)}{\partial \psi_k} \tag{10.30}$$

$$T_{rr}(\boldsymbol{x}) = \frac{1}{r^2}\sum_{k=1}^{K} d_k \sum_n (2n+1)(n+1)(n+2) B_n \mu^{n-1} P_n(\psi_k) \tag{10.31}$$

Substituting the specific B_n from Table 7.2 yields the fundamental observation equations:

$$\boldsymbol{L} = \{F(\boldsymbol{x}_i)\}^T = \boldsymbol{A}\{d_k\}^T + \boldsymbol{\varepsilon} \quad (i = 1, \cdots, M; k = 1, \cdots, K) \tag{10.32}$$

where M is the number of observations, K is the number of SRBF centers, and:

$\boldsymbol{L} = \{F(\boldsymbol{x}_1), \cdots, F(\boldsymbol{x}_M)\}^T$: Vector of observed (residual) field elements.

$\boldsymbol{d} = \{d_1, \cdots, d_K\}^T$: Vector of unknown SRBF coefficients.

$\boldsymbol{A}$: The $M \times K$ design matrix, containing the SRBF functions.

$\boldsymbol{\varepsilon}$: The $M \times 1$ observation error vector

● Technical Constraint: Uniform Action Distance

To ensure spatial consistency in the approximation quality, a critical requirement in constructing Eq. (10.32) is that all SRBF centers share an identical Action Distance (or Influence Radius) $d\,r$.

○ Definition: An observation at $\boldsymbol{x}_i$ is influenced only by SRBF nodes k satisfying $\psi_{i,k} \leq dr/\mathcal{R}$.

○ Implication: The support domain of SRBFs is truncated uniformly. This parameter $d\,r$ is conceptually equivalent to the integration radius in spatial local gravity field methods.

7.10.4 Parameter Estimation via Grouped Synergistic Adjustment of Multi-Source Heterogeneous Observations

Observations of gravity field elements exhibit distinct spatial distributions and sensitivity characteristics relative to Spherical Radial Basis Function (SRBF) coefficients. Consequently, the design matrices (sensitivity matrices) within their respective observation equations often possess disparate structural features. Formulating separate normal equations for each observation type and combining them through standard Variance Component Estimation (VCE) frequently results in unstable solutions for the SRBF coefficients due to ill-conditioning.

To address this numerical instability, a Grouped Synergistic Adjustment strategy is employed:

(a) System Grouping: Observation equations are partitioned into distinct groups based on their sensitivity patterns (design matrix $\boldsymbol{A}$) to SRBF coefficients. Observations across different groups are statistically independent, while the design matrices within a single group exhibit homogeneity. Each partition constitutes a distinct Observation System.

(b) Normalization: Normal equations for each system are formed via the Least Squares Principle and subsequently normalized to eliminate magnitude discrepancies arising from differing physical units or sensitivities.

(c) Weighted Combination: System weights are assigned based on observational quality. The normalized normal equations are weighted and summed to form a Combined Normal Equation:

$$\sum_k \left(\frac{w_k}{Q_k}\boldsymbol{A}_k^{\mathrm{T}}\boldsymbol{P}_k\boldsymbol{A}_k\right)\{d_k\}^{\mathrm{T}} = \sum_k \left(\frac{w_k}{Q_k}\boldsymbol{A}_k^{\mathrm{T}}\boldsymbol{P}_k\boldsymbol{L}_k\right) \tag{10.34}$$

where:

k =1,⋯,K : Index of the observation system; K denotes the total number of system groups..

$\boldsymbol{d} = \{d_k\}^{\mathrm{T}}$: Vector of unknown SRBF coefficients.

$\boldsymbol{A}_k, \boldsymbol{P}_k, \boldsymbol{L}_k$: Design matrix, weight matrix, and observation vector for system k , respectively.

Q_k: Normalization parameter, defined as the Root Mean Square (RMS) of the diagonal elements of $\boldsymbol{A}_k^{\mathrm{T}}\boldsymbol{P}_k\boldsymbol{A}_k$. This factor mitigates scale differences in sensitivity between disparate observation systems.

w_k: System weight, reflecting the relative quality of system k compared to others.

Key Properties:

● Independence: The internal weights P_{ki} affect only system k . Normalization via Q_k ensures that systems with sparse observations do not lose sensitivity when combined with dense systems.

● System Weight Determination: The weights w_k are estimated via a simplified Iterative VCE process:

○ Initialization: Set $w_k = 1$ and solve for preliminary SRBF coefficient vector $\boldsymbol{d}$.

○ Variance Estimation: Compute the posteriori variance σ_k^2 for each system using observation residuals.

○ Influence Propagation: Estimate the influence of σ_k^2 on the unknowns (approximated via error propagation):

$$\tilde{\sigma}_{k,s}^2 = \frac{1}{\left(\boldsymbol{A}_k^T\boldsymbol{A}_k\right)_s}\sigma_k^2, \quad w_k = \left(\sum_s \tilde{\sigma}_{k,s}^2\right)^{-1} \tag{10.35}$$

where s indexes the SRBF coefficients.

○ Iteration: Update w_k and resolve. This process typically converges within one iteration.

Note: One may analyze the variance function curves $\tilde{\sigma}_{k,s}^2$ with s as the independent variable across different systems to optimize system weights based on specific sensitivity requirements.

7.10.5 Zero-Constraint Method for SRBF Coefficients at Distant Outer Boundaries

In local gravity field approximation, Outer Boundary Constraints are necessary to suppress edge effects and stabilize the solution in regions with sparse data.

Methodology:

$$[\boldsymbol{A}^T\boldsymbol{P}\boldsymbol{A} + \epsilon\boldsymbol{\Xi}]\{d_k\}^T = \boldsymbol{A}^T\boldsymbol{P}\boldsymbol{L} \tag{10.33}$$

where:

$\boldsymbol{\Xi}$: A diagonal constraint matrix. $\Xi_{vv} = 1$ if node v is at or outside the boundary of target region; otherwise 0.

ϵ: A scaling factor, defined as the reciprocal of the RMS of the diagonal elements of $\boldsymbol{A}^T\boldsymbol{P}\boldsymbol{A}$, ensuring numerical balance between data and constraints.

Advantages: The addition of boundary conditions can weaken the need for Tikhonov-type regularization, which might otherwise distort the analytical relationships between field elements. Thus, the intrinsic functional relationships derived from potential theory are preserved.

7.10.6 Cumulative SRBF Approximation Scheme for Residual Gravity Field elements

From a signal processing perspective, the target field element is effectively the convolution of the observed field element and the SRBF filter kernel. When the target and observed elements differ in type (e.g., approximating gravity anomalies from gravity gradients), a single SRBF function often fails to simultaneously match the spectral center and bandwidth of both elements. This mismatch can lead to spectral leakage, degrading the fidelity of the target field reconstruction. Furthermore, SRBF approximation performance depends on multiple factors beyond the Bjerhammar sphere burial depth $\mathcal{R}$ (or bandwidth parameter $\mu = \mathcal{R}/r$), including:

- The specific SRBF kernel type (Poisson, Radial multipole kernel, etc.).
- The spectral truncation limits (n_{min}, n_{max}).
- The Reuter grid level (Q) and node distribution.
- The effective action distance.

Consequently, optimizing SRBF coefficients solely by tuning the bandwidth parameter μ is insufficient to guarantee an optimal solution.

(1) Proposed Solution: Cumulative SRBF Approximation

To address this limitation, we propose a Cumulative SRBF Approximation Scheme based on the linear additivity of gravity field functionals. Unlike traditional methods that seek a single optimal μ , this scheme employs a multi-step iterative strategy:

- Multi-Spectral Fusion: Each approximation step utilizes SRBFs with distinct spectral characteristics (different centers and bandwidths).
- Parameter Flexibility: Individual steps do not require a fixed, globally optimal Bjerhammar radius $\mathcal{R}$ or μ .
- Signal Resolution: By accumulating contributions from multiple spectral bands, the method can fully resolve the target field's signal content, mitigate spectral leakage, and achieve superior approximation accuracy.

(2) Algorithmic Interpretation

Each step in the Cumulative SRBF method functions equivalently as a Remove-Restore process:

- Remove: The residual field from the previous step serves as the input.
- Restore: The current SRBF approximation models a specific spectral band of the residuals.
- Update: The new approximation is added to the cumulative model, updating the reference field for the next iteration.

This approach ensures that complex gravity field signals, which cannot be captured by a single scale parameter, are reconstructed progressively and robustly.

(3) Quantitative Criteria for Single-Step Effectiveness

The validity of each iteration within the cumulative scheme is governed by two simple and intuitive criteria:

● Spatial Regularity & Minimization: The target field element grid should remain spatially continuous and differentiable, and the standard deviation of residual observations is as small as possible.

● Convergence Behavior: As cumulative steps proceed, the statistical mean of the residual observations must converge toward zero without exhibiting significant sign reversals (indicative of over-correction or instability).

(4) Distinctive Technical Features of the PAGravf4.5 SRBF Module

(a) Strict Analytical Consistency and Error Immunity:

The approximation scheme strictly adheres to the intrinsic analytical functional relationships between gravity field elements. The approximation performance is mathematically decoupled from random observational errors, guaranteeing the internal consistency of the physical-mathematical model.

(b) Direct Full-Space, All-Element Modeling Without Traditional Pre-processing:

Capable of directly utilizing multi-source heterogeneous observations to construct all-element gravity field models on or outside the geoid. No traditional gravity reduction, upward/downward continuation, or gridding interpolation is required, thereby eliminating signal attenuation and non-analytical distortions at the source.

(c) Robust Fusion of Sparse observations:

Exhibits superior capability in leveraging and fusing sparse high-precision observation data (e.g., limited astronomical vertical deflections or GNSS-leveling sites).

(d) Advanced Quality Control and Performance Assessment:

Equipped with high-precision mechanisms for detecting observational gross errors, quantitatively assessing external accuracy metrics, and comprehensively monitoring and optimizing computational performance.